

Contents lists available at [ScienceDirect](https://www.sciencedirect.com)

Chemical Engineering Research and Design

journal homepage: www.elsevier.com/locate/cherd


Evaluating the possibility of high-pressure desorption of CO₂ via volatile co-solvent injection

Ricardo R. Wanderley, Hanna K. Knuutila*

Department of Chemical Engineering, Norwegian University of Science and Technology (NTNU), NO-7491 Trondheim, Norway

ARTICLE INFO

Article history:

Received 25 November 2020

Received in revised form 4 March 2021

2021

Accepted 11 March 2021

Available online 17 March 2021

Keywords:

CO₂ captureCO₂ desorptionCO₂ stripping

High-pressure

Water-lean solvent

ABSTRACT

This work evaluates the possibility of employing a volatile co-solvent injection for recovering CO₂ from loaded monoethanolamine at 120 °C under pressures above those achievable through regular desorption processes. This co-solvent would be fed directly into the reboiler, percolating the column and delivering higher operational pressures without significantly affecting the chemical equilibrium between CO₂ and the amine. Removal of this co-solvent would be required before the lean amine is recirculated to the absorber. A shortcut methodology for screening possible co-solvent candidates is presented, and MESH calculations of hypothetical stripping processes employing the high-pressure desorption approach are performed to illustrate the expected behavior of these systems. Pressures above 500 kPa are theoretically obtainable through the use of co-solvents which are less volatile than CO₂ but that are still gases at 25 °C and 101.325 kPa, such as isobutane and dimethyl ether. These co-solvents will leave the desorber fractionated between the distillate and the bottom product, thus requiring two additional separation process for recovery. Less volatile solvents will concentrate at the bottom stages of the desorber, while more volatile solvents will flow straight through the column all the way up to the distillate without effectively delivering pressures as high as desired. In other words, this methodology results in a delicate optimization problem of finding ideal volatilities and operational conditions. Though no detailed energy analysis is performed in this preliminary assessment, we have identified a promising opportunity for CO₂ production at higher pressures and enumerated the issues one should be concerned with when looking further into high-pressure desorption.

© 2021 The Authors. Published by Elsevier B.V. on behalf of Institution of Chemical Engineers. This is an open access article under the CC BY license (<http://creativecommons.org/licenses/by/4.0/>).

1. Introduction

Chemical absorption via aqueous amine solvents is an established technology for CO₂ recovery from gaseous streams such as natural gas, syngas and flue gas (Rochelle, 2009). In general terms, this technique relies on manipulating the temperature-dependent chemical equilibrium between amine and CO₂ for capturing CO₂ at low temperatures in an absorber column and releasing it at high temperatures in a stripper column. While most cycles work with the absorber designed to operate at about 30–40 °C regardless of the solvent (unless it is a particularly volatile one, such as the Amisol® solvent (Kriebel, 1984), and ignoring the temperature increases brought by the exothermicity of

CO₂ absorption), the temperature of the stripper is neatly delimited by the thermal degradation features of the amine (Rochelle, 2012, 2016). In the particular case of aqueous monoethanolamine (MEA), the maximum operational temperature of the reboiler is around 120 °C (Vega et al., 2014). Davis and Rochelle (2009) have demonstrated that, for each 17 °C increase in temperature, MEA degradation rates accelerate four-fold. After being recovered, CO₂ must be compressed to up to 6–10 MPa for transportation and injection (Wang et al., 2019). It has been shown that higher desorber pressures result in lower compression duties to achieve such transportation conditions together with lower regeneration duties (Oyeneke and Rochelle, 2007). And yet, reboiler pressure and temperature are intrinsically interlinked through the vapor-liquid equilibrium (VLE) behavior of the aqueous amine solvent. If one wants to obtain a lean solvent with a determined concentration of CO₂ below a determined temperature threshold, the pressure cap is inherently fixed.

* Corresponding author.

E-mail address: hanna.knuutila@ntnu.no (H.K. Knuutila).<https://doi.org/10.1016/j.cherd.2021.03.011>0263-8762/© 2021 The Authors. Published by Elsevier B.V. on behalf of Institution of Chemical Engineers. This is an open access article under the CC BY license (<http://creativecommons.org/licenses/by/4.0/>).

The present study proposes an alternative to break this deadlock, which is the injection of a volatile co-solvent directly to the reboiler. The addition of a new component introduces another degree of freedom to the stripper and allows for CO₂ recovery at higher pressures under the same temperature threshold of 120 °C. This co-solvent would then be recovered from the product streams of the desorber, with the chosen recovery technology being dependent on whether the co-solvent leaves as a gas together with CO₂ or as a liquid mixed with the lean amine in the bottom product (or alternatively fractioned between both streams). In any case, our initial concept is that this co-solvent should not be allowed to return to the absorber column with the amine, where it might derange absorption capacities and rates as shown in our previous studies (Wanderley et al., 2019, 2020) and additionally complicate emission control systems.

This is not an entirely new proposal. A similar concept can be found in the work of Tobiesen and Svendsen (2006). However, that study was fixated on the idea that one might be able to decrease reboiler duties with the addition of a volatile co-solvent. As shown by the authors, that is not entirely feasible. Conversely, direct stripping of the amine with a co-solvent vapor stream (pentane) has been analyzed by Yang et al. (2020) and evaluated in terms of regeneration duties, with no assessment of the possibility of recovering CO₂ at higher pressures. Our approach is slightly different from these works: we do not intend to decrease regeneration duties with this process modification, and fully accept that those will probably increase. Nevertheless, if the addition of a volatile co-solvent can attain enough pressure, then this increase in regeneration duties might be offset by a decrease in compression duties.

Process design and simulation are the tools upon which this work will rely to evaluate the consequences of employing a volatile co-solvent for high-pressure desorption. In that, the approach adopted here is very similar to that employed previously in the assessment of hypothetical water-lean solvents for CO₂ capture (Wanderley and Knuutila, 2020). The way in which this study is structured is the following:

- i The methodologies to calculate VLE behavior and solve mass and energy balances in a desorber operating at steady state are described in Sections 2.1 and 2.3. Section 2.2 employs the VLE calculation to propose a shortcut methodology for evaluating candidate co-solvents with the aid of a simple database containing Antoine parameters of several chemical compounds.
- ii Shortcut evaluations of possible volatile co-solvents are carried out in Section 3.1. A pattern is clearly identified in which most plausible candidates are light, flammable organic compounds.
- iii Desorber operations with the addition of a series of co-solvents that are liquid at 101.325 kPa and 25 °C are simulated and analyzed in Section 3.2. These are co-solvents of moderate volatility well exemplified by the series of furans.
- iv Desorber operations with the addition of a series of co-solvents that are gas at 101.325 kPa and 25 °C are simulated and analyzed in Section 3.3. These so-called *hyper volatile co-solvents* are represented by dimethyl ether and isobutane.

Despite the target of this process modification being the reduction of total power usage in the CO₂ capture plant, we must remark that this study does not intend to carry out a proper energetic or exergetic evaluation of high-pressure desorption as a whole. There are presently many unknowns regarding the process, and the methodology employed here is too simplistic to correctly estimate the costs of co-solvent separation from the lean amine or even correctly evaluate if the liquid product will be a single-phase or a biphasic stream. However, this methodology is able to predict and identify patterns and phenomena that might be observed when employing co-solvent injection for high-pressure desorption. Therefore, this is a valuable preliminary study in a possible future CO₂ recovery technology.

2. Methodology

2.1. Vapor-liquid equilibrium

For the following series of developments, we have employed an equilibrium approach that conceals the reactions between CO₂, MEA and water. This implies that mass balances throughout the column will keep track of MEA concentrations while concealing the fact that the 'MEA' subscript actually stands for a mixture of free MEA, protonated MEA and MEA carbamate. Similarly, mass balances will keep track of 'CO₂' concentrations in the liquid phase while concealing that these values apply for molecular CO₂ plus MEA carbamate and bicarbonate molecules. One could point out that, e.g., this means we are counting MEA carbamate twice. In reality, what matters is that, through consistent checking of mass balances and equilibrium calculations, all mass transfer phenomena in the desorber are thoroughly accounted for.

The vapor-liquid equilibrium of CO₂ in the solvent is given by the soft model, which correlates the CO₂ partial pressure in the vapor phase in kPa (p_{CO_2}) with CO₂ loading in mol CO₂/mol amine (α) and temperature (T) in K (Aronu et al., 2014). For aqueous MEA 30%wt., the soft model equation is defined as Eqs. (1a)–(1d).

$$\ln(p_{CO_2}) = 1.8 \cdot \ln(\alpha) + k_1 + \frac{10}{1 + k_2 \cdot \exp(k_3 \cdot \ln(\alpha))} \quad (1a)$$

$$k_1 = -9155.955 \cdot \frac{1}{T} + 28.027 \quad (1b)$$

$$k_2 = \exp\left(-6146.18 \cdot \frac{1}{T} + 15\right) \quad (1c)$$

$$k_3 = -7527.0376 \cdot \frac{1}{T} + 16.942 \quad (1d)$$

Meanwhile, the vapor-liquid equilibria of water, MEA and the co-solvent are calculated by Raoult's law in conjunction with Dalton's law, Eq. (2). In Eq. (2), p is the total pressure, p_i^{sat} is the saturation pressure of component i , and y_i and x_i are respectively the molar fractions of component i in the vapor and in the liquid phase.

$$p \cdot y_i = p_i^{sat} \cdot x_i \quad (2)$$

The concentrations of amine and water before the addition of the co-solvent are specified by the fact that we are operating with aqueous MEA 30%wt., so that initially $x_{MEA} = 0.1122$ and $x_{H_2O} = 0.8878$. The addition of a co-solvent simply implies renormalizing these molar fractions. We have introduced a factor f_{COS} which accounts for how much co-solvent is solubilized in the liquid phase as a ratio of the water content of the fresh solvent, Eq. (3).

$$f_{COS} = \frac{x_{COS}}{x_{H_2O}^{fresh}} \quad (3)$$

Additionally, the absorption of CO₂ brings a fourth component to the mixture, and the loading α can be employed as a second renormalization factor. Renormalizing the molar fractions of water, MEA, co-solvent and CO₂ entails Eqs. (4a)–(4d).

$$x_{H_2O} = \frac{x_{H_2O}^{fresh}}{(1 + f_{COS}) \cdot x_{H_2O}^{fresh} + (1 + \alpha) \cdot x_{MEA}^{fresh}} \quad (4a)$$

$$x_{\text{MEA}} = \frac{x_{\text{MEA}}^{\text{fresh}}}{(1 + f_{\text{CO}_2}) \cdot x_{\text{H}_2\text{O}}^{\text{fresh}} + (1 + \alpha) \cdot x_{\text{MEA}}^{\text{fresh}}} \quad (4b)$$

$$x_{\text{CO}_2} = \frac{f_{\text{CO}_2} \cdot x_{\text{H}_2\text{O}}^{\text{fresh}}}{(1 + f_{\text{CO}_2}) \cdot x_{\text{H}_2\text{O}}^{\text{fresh}} + (1 + \alpha) \cdot x_{\text{MEA}}^{\text{fresh}}} \quad (4c)$$

$$x_{\text{CO}_2} = \frac{\alpha \cdot x_{\text{MEA}}^{\text{fresh}}}{(1 + f_{\text{CO}_2}) \cdot x_{\text{H}_2\text{O}}^{\text{fresh}} + (1 + \alpha) \cdot x_{\text{MEA}}^{\text{fresh}}} \quad (4d)$$

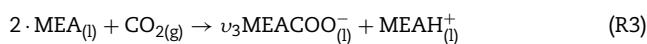
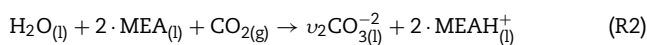
The previous Eqs. (4a) to (4d) are useful for calculating liquid phase molar fraction concentrations for mass balance purposes. However, they might be inadequate for vapor pressure purposes, i.e. for using Eq. (2), particularly in the case of water and MEA. The reason is that, as CO_2 is consumed by the liquid phase and the loading increases, the effective molar fractions of amine and water will be reduced. If one were to consider the reaction between two molecules of amine with one of CO_2 to generate one molecule of carbamate and protonated amine, the relationship between CO_2 loading and the number of mols of amine would be pretty straightforward, Eq. (5a). Additionally, the concentration of water in the liquid phase would be independent of loading, Eq. (5b).

$$n_{\text{MEA}}^{\text{eff}} = n_{\text{MEA}}^{\text{app}} \cdot (1 - 2 \cdot \alpha) \quad (5a)$$

$$n_{\text{H}_2\text{O}}^{\text{eff}} = n_{\text{H}_2\text{O}}^{\text{app}} \quad (5b)$$

The problem with Eq. (3) is that it does not apply for higher CO_2 loadings, where the participation of water in the reaction mechanism becomes more relevant through the formation of bicarbonate and carbonate. In that case, Eqs. (4a) and (4b) become inadequate.

Wong et al. (2016) have published Raman spectroscopic data for the speciation of the reactive water–MEA– CO_2 milieu at 40 °C. This data was employed to fit the degrees of advancement (ν , where ν is a vector with components ν_1 , ν_2 and ν_3) of the following set of reactions as a function of α :



This set of equations ignores the presence of molecular CO_2 in the liquid phase, which is nonetheless quite small under loadings of $\alpha = 0.6$ (Wong et al., 2016), especially at higher temperatures. Once the values of ν are found, the number of free water and MEA molecules can be calculated as a function of α . Notice that, through reactions (R1)–(R3), the number of molecules in the liquid phase is never modified. Therefore, Eqs. (5a) and (5b) should be valid both for the calculation of mole numbers as for the calculation of molar fractions, as no renormalization is necessary. In the case of the addition of a co-solvent, the apparent concentration of water and MEA can be conveniently calculated by Eqs. (6a) and (6b).

$$x_{\text{H}_2\text{O}}^{\text{app}} = \frac{x_{\text{H}_2\text{O}}^{\text{fresh}}}{(1 + f_{\text{CO}_2}) \cdot x_{\text{H}_2\text{O}}^{\text{fresh}} + x_{\text{MEA}}^{\text{fresh}}} \quad (6a)$$

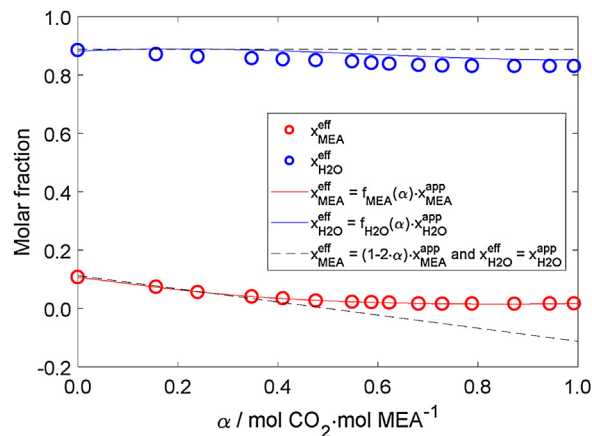


Fig. 1 – Molar fractions of water and MEA as a function of loading, derived from data for aqueous MEA 30%wt. at 40 °C obtained by Wong et al. (2016).

$$x_{\text{MEA}}^{\text{app}} = \frac{x_{\text{MEA}}^{\text{fresh}}}{(1 + f_{\text{CO}_2}) \cdot x_{\text{H}_2\text{O}}^{\text{fresh}} + x_{\text{MEA}}^{\text{fresh}}} \quad (6b)$$

The fitting of ν has been performed by the particle swarm optimization described in past works (Evjen et al., 2019; Skylogianni et al., 2019), and with this fitting we were able to obtain an expression correlating the effective $x_{\text{H}_2\text{O}}$ and x_{MEA} to α , Eqs. (7a) and (7b). A visual interpretation of these equations is shown in Fig. 1, where $f_{\text{MEA}}(\alpha)$ is the expression shown in Eq. (7a) and $f_{\text{H}_2\text{O}}(\alpha)$ is the expression shown in Eq. (7b).

$$x_{\text{MEA}}^{\text{eff}} = x_{\text{MEA}}^{\text{app}} \cdot \exp(-0.0451 - 1.9910 \cdot \alpha - 3.4911 \cdot \alpha^2 + 3.6741 \cdot \alpha^3) \quad (7a)$$

$$x_{\text{H}_2\text{O}}^{\text{eff}} = x_{\text{H}_2\text{O}}^{\text{app}} \cdot \exp(-0.0069 + 0.0971 \cdot \alpha - 0.2983 \cdot \alpha^2 + 0.1665 \cdot \alpha^3) \quad (7b)$$

Fig. 1 shows that, for loadings below $\alpha = 0.4$, the approximation that two molecules of MEA are consumed for each molecule of CO_2 absorbed is actually fine. This can be seen in how the bold red and blue lines approach the dashed black lines, which account solely for the carbamate mechanism. This mechanism alone is not enough to explain how water and amine are consumed at higher loadings, and Eqs. (7a) and (7b) become more relevant.

With Eqs. (6a), (6b), (7a) and (7b), Eq. (2) can be rewritten as Eqs. (8a) and (8b). Eq. (8c) shows how to calculate the partial pressure of the co-solvent in the vapor phase. In these expressions, we are also making it clear that the fresh solvent, by definition, consists solely of water and MEA, i.e. $x_{\text{H}_2\text{O}} = 1 - x_{\text{MEA}}$. The consequence is that, if one settles for an initial concentration of aqueous unreacted MEA, a CO_2 loading, a co-solvent factor f_{CO_2} and a temperature, the equilibrium system is completely defined. As mentioned before, the CO_2 partial pressure comes from Eq. (1a), which depends only on loading and temperature.

$$p_{\text{H}_2\text{O}} = p_{\text{H}_2\text{O}}^{\text{sat}} \cdot x_{\text{H}_2\text{O}}^{\text{eff}}$$

$$= p_{\text{H}_2\text{O}}^{\text{sat}} \cdot \frac{1 - x_{\text{MEA}}^{\text{fresh}}}{(1 + f_{\text{COS}}) \cdot \left(1 - x_{\text{MEA}}^{\text{fresh}}\right) + x_{\text{MEA}}^{\text{fresh}}} \cdot f_{\text{H}_2\text{O}}(\alpha) \quad (8a)$$

$$p_{\text{MEA}} = p_{\text{MEA}}^{\text{sat}} \cdot x_{\text{MEA}}^{\text{eff}}$$

$$= p_{\text{MEA}}^{\text{sat}} \cdot \frac{x_{\text{MEA}}^{\text{fresh}}}{(1 + f_{\text{COS}}) \cdot \left(1 - x_{\text{MEA}}^{\text{fresh}}\right) + x_{\text{MEA}}^{\text{fresh}}} \cdot f_{\text{MEA}}(\alpha) \quad (8b)$$

$$p_{\text{COS}} = p_{\text{COS}}^{\text{sat}} \cdot x_{\text{COS}}^{\text{eff}} = p_{\text{COS}}^{\text{sat}} \cdot \frac{f_{\text{COS}} \cdot \left(1 - x_{\text{MEA}}^{\text{fresh}}\right)}{(1 + f_{\text{COS}}) \cdot \left(1 - x_{\text{MEA}}^{\text{fresh}}\right) + x_{\text{MEA}}^{\text{fresh}}} \quad (8c)$$

As a sidenote: Eqs. (7a) and (7b) are useful as a stepping stone for calculating vapor pressures via Eqs. (8a)–(8c). However, we must highlight the fact that they introduce a ‘destruction’ of amine and water species with increased CO₂ loadings that would be rather problematic for keeping mass balances throughout the column in case they were used for evaluating liquid phase concentrations instead of Eqs. (4a) and (4b). In other words, the set of Eqs. (4a)–(4d) has been designed so that the sum of all molar fractions in the liquid phase is always $\sum x_i = 1$, whereas Eqs. (7a) and (7b) do not obey this rule. Therefore, one must be careful to distinguish where Eqs. (7a) and (7b) are applicable and where they are not.

The saturation pressure of water, amine and co-solvent can be calculated through the Antoine equation, Eq. (9). Eq. (9) is written in a form wherein the temperature is given in K and the saturation pressure is delivered in kPa, though its parameters A_i , B_i and C_i have been obtained in a database which requires T in °C and p^{sat} in mmHg. The Antoine parameters for water, MEA and some candidate co-solvents are given in the Appendix A of this study.

$$\log_{10} \left(\frac{p_i^{\text{sat}}}{0.13332} \right) = A_i - \frac{B_i}{C_i + T - 273.15} \quad (9)$$

Though this formulation of the vapor-liquid equilibrium problem might seem convoluted, it is actually very convenient. While Eqs. (4a)–(4d) offer a simple way of keeping track of the flow rates of all components in the liquid phase, Eqs. (1a) and (8a)–(8c) offer a way of keeping track of flow rates in the vapor phase. The application of these formulae will be shown in the following Sections 2.2 and 2.3. However, to finish this section, it might be interesting to list the assumptions taken during the derivation of these equations.

- i Both Raoult’s and Dalton’s laws are valid for free unreacted molecules, which is reasonable due to the relatively low pressures and high temperatures. This means that fugacity coefficients and activity coefficients are always unity, regardless of loading;
- ii The dependency between CO₂ loading and CO₂ partial pressure does not change with the addition of the co-solvent. This can be argued to not be true, see for example Wanderley et al. (2020);

- iii The addition of the co-solvent does not bring neither a new reaction with CO₂ nor a new reaction with MEA, i.e. the co-solvent must be perfectly inert;
- iv Additionally, the dependency between CO₂ loading and CO₂ partial pressure follows the model of Aronu et al. (2014) parametrized for aqueous 30%wt. MEA regardless of the fact that the proportions of water and amine are allowed to vary in our calculations;
- v The co-solvent is deemed to be soluble in the aqueous phase. No second liquid phase formation is considered. A compendium of water miscibility of many of the co-solvents explored in this work can be found in Yaws (2003), though amine speciation will have an impact in liquid-liquid equilibria as seen in the case of biphasic water-lean solvents (Zhang et al., 2012, 2019; Zhuang et al., 2016);
- vi The speciation data obtained by Wong et al. (2016) for aqueous 30%wt. MEA at 40 °C is valid for varying water-amine concentrations even at high desorber temperatures.

Of these assumptions, we believe that (i), (iv) and (vi) are relatively inconsequential. Assumptions (ii), (iii) and (v) are slightly more problematic, and they are discussed again in Section 3.1.

2.2. Shortcut evaluation of co-solvent candidates

With the equations shown in the Section 2.1, the evaluation of co-solvent candidates is very straightforward. If one fixes the concentration of aqueous unreacted MEA (MEA 30%wt. implies $x_{\text{MEA}} = 0.1122$), the desired lean loading of the solvent and the reboiler temperature, each f_{COS} will result in a different total pressure p . This is shown in Eq. (10), which relies on the formulae presented in Section 2.1.

$$p = p_{\text{H}_2\text{O}} \left(x_{\text{MEA}}^{\text{fresh}}, \alpha, f_{\text{COS}}, T \right) + p_{\text{MEA}} \left(x_{\text{MEA}}^{\text{fresh}}, \alpha, f_{\text{COS}}, T \right) + p_{\text{CO}_2} \left(\alpha, T \right) + p_{\text{COS}} \left(x_{\text{MEA}}^{\text{fresh}}, \alpha, f_{\text{COS}}, T \right) \quad (10)$$

In Section 3.1, we perform a screening of possible co-solvent candidates by fixing a desired lean loading of $\alpha = 0.2$ mol CO₂/mol MEA, a reboiler temperature of 120 °C and a $f_{\text{COS}} = 0.1$ mol co-solvent/mol water. For Sections 3.2 and 3.3, f_{COS} is allowed to vary while the remainder process specifications are kept just as in Section 3.1. The important aspect of this analysis is that the only parameters directly depending on the nature of the co-solvent are the three Antoine coefficients used to calculate the co-solvent saturation pressure, Eq. (9). By compiling a comprehensive database of Antoine coefficients, one is able to carry out this shortcut evaluation for a large array of co-solvent candidates. An example of this procedure is shown in Section 3.1.

However, one must notice that this shortcut methodology does not directly indicate how much co-solvent must be injected in the process. The operational conditions of the desorber (for example, its reflux and boil-up ratios, R_D and R_B) affect the liquid and vapor flow rates entering and leaving the reboiler. These flow rates cannot be obtained without a full assessment of the stripper column. As a result, there is no straightforward correlation between the required molar fraction of co-solvent in the reboiler liquid phase ($x_{\text{COS}} = f_{\text{COS}} \times x_{\text{H}_2\text{O}}$) and the molar flow rate of co-solvent that must be injected to the column (F_{COS}). For co-solvents that are not hyper volatile,

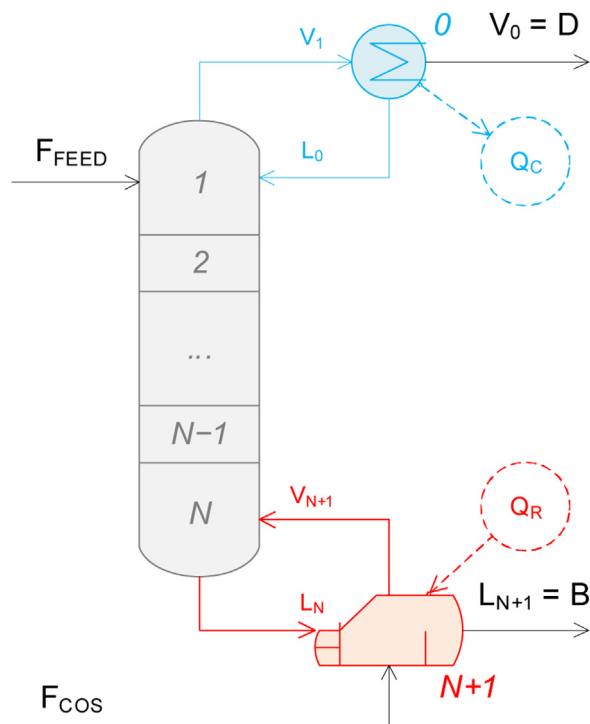


Fig. 2 – Schematic representation of the desorber with co-solvent injection.

it is a suitable educated guess to estimate that all co-solvent injected ends up in the reboiler liquid phase, i.e. $F_{\text{COS}} \approx f_{\text{COS}} \times F_{\text{H}_2\text{O,FEED}}$. For hyper volatile co-solvents, the complete desorber modelling is even more essential for understanding the performance of the stripper employing co-solvent injection.

2.3. Desorber modelling with MESH algorithm

The acronym MESH stands for Material, Equilibrium, Summation and Heat (Wagialla and Soliman, 1993). Modelling a desorber with a MESH algorithm implies solving all material and energy balances while applying vapor-liquid equilibrium equations to each stage. In our previous work, we have employed a MESH procedure to model an absorber operating with water-lean solvents (Wanderley and Knuutila, 2020). The procedure adopted in the present study is quite similar to that one. A good description of how to quickly implement and solve MESH equations is given by Steffen and Silva (2017).

A schematic drawing of the proposed desorption column is shown in Fig. 2.

The desorber is modelled as having $N + 2$ equilibrium stages, meaning it has one condenser, one reboiler and N inner stages. The condenser is a partial condenser where an amount of energy Q_C is removed from the stage and a vapor stream $V_0 = D$ is obtained as distillate. The reboiler is a partial reboiler where an amount of energy Q_R is added to the stage and a liquid stream $L_{N+1} = B$ is obtained as bottom product. The rich amine, which is aqueous MEA 30%wt. with a loading of $\alpha = 0.5$ mol CO_2 /mol MEA, is fed to the first stage of the column at 105°C and a molar flow rate $F_{\text{FEED}} = 1$ kmol/h. A stream of pure co-solvent is fed directly into the reboiler at 120°C and a molar flow rate F_{COS} . Essentially the absolute values of F_{FEED} and F_{COS} are less interesting for simulation purposes than their values relative to each other. The column is modelled as being perfectly isobaric.

Notice that vapor-liquid equilibrium demands that the pressure of the reboiler be fixed once its composition and temperature are defined. Our process requirements are already specifying a maximum reboiler temperature and a desired solvent lean loading. Therefore, if one wants to modify the operational pressures of the process, the most straightforward way of doing so is by shifting the concentrations directly in the reboiler. This is why we propose the co-solvent addition precisely into that stage. Moreover, since this co-solvent is volatile, an injection anywhere else in the column would require an increased level of co-solvent condensation in order to affect the vapor-liquid equilibrium in the reboiler, which would imply increasingly high condenser duties, recirculation rates, and reboiler duties.

Solving this model implies solving the mass balances for each one of the four components across the $N + 2$ stages and then solving the energy balances at each stage. This means solving $5 \times (N + 2)$ equations. Additionally, to be able to adjust the operational specifications of the desorber, we are fixing one desired variable at the top and one at the bottom. At the bottom of the column, we have specified that the lean loading of the solvent coming out must be $\alpha = 0.2$ mol CO_2 /mol MEA. At the top, we had to make a decision between specifying the temperature of the condenser or the CO_2 concentration in the distillate. We have ultimately decided to specify the temperature of the condenser.

As mentioned previously, the column is modelled as having the same pressure across all stages. This pressure has been initially set as that given by Eq. (10), i.e. as that evaluated by the shortcut method, being essentially dependent on the co-solvent flow rate F_{COS} (or rather of the estimated f_{COS} at the reboiler). Due to the shortcomings of this rough calculation, it happened often that the MESH algorithm, when fully solved, returned a temperature at the reboiler slightly superior or inferior to 120°C . We have added a small iteration loop to re-estimate the column pressure p with the intent of meeting the reboiler temperature of 120°C within a margin of $\pm 0.05^\circ\text{C}$. Therefore, the reboiler temperature is also a specification of the process, although it is being manipulated indirectly through the updating of p .

The energy balances in this study have been performed in the same way as those of our previous work (Wanderley and Knuutila, 2020). The heat of vaporization of water, amine and co-solvent has been recovered from the Antoine expression Eq. (9) through the use of the Clausius-Clapeyron relationship. The heat of vaporization of CO_2 has been considered constant at $-\Delta H^{\text{abs}} = 85$ kJ/mol CO_2 following the experimental data obtained by Kim et al. (2014) and Wanderley et al. (2020) among others. The gas heat capacity has been calculated using temperature-dependent parameters provided by Yaws (2003) and, in the case of nitrogen, by Coker (2007). We have taken the decision to employ only gas heat capacities in this work. This can be done since, following thermodynamic consistency, the heat demanded to change the temperature of a liquid between T_1 and T_2 is the heat demanded to vaporize the liquid at T_1 , plus the heat to shift the temperature of the gas from T_1 to T_2 , plus the heat demanded to condense the gas at T_2 . As such, this approach allows us to avoid getting bogged on having to make assumptions regarding how to calculate the heat capacity of electrolytic solutions. An obvious criticism is that this is a highly simplified way of performing calculations. Nevertheless, this methodology ensures that thermodynamic consistency is achieved in the energy balances. Moreover, the goal of this study is not to come up with energy values for the

performance of high-pressure desorption systems, but simply to identify patterns and behaviors when employing volatile co-solvents. For the sake of obtaining these patterns in a timely and comprehensive manner, we believe that our approach is good enough to solve the MESH equations.

To facilitate the discussion of our results, we will introduce some useful parameters. These are the reflux ratio R_D , Eq. (11a), and the boil-up ratio R_B , Eq. (11b). Additionally, we will discuss the condenser and reboiler duties Q_C and Q_R in terms of the amount of CO_2 recovered in the distillate, i.e. these duties will be given in MJ/kg CO_2 recovered instead of, for example, MJ/h.

$$R_D = \frac{L_0}{D} \quad (11a)$$

$$R_B = \frac{V_{N+1}}{B} \quad (11b)$$

The stripper has been proposed as having 5 inner equilibrium stages, meaning 5 + 2 in total. In our analyses, the temperature of the reboiler of 120 °C and the lean solvent loading $\alpha = 0.2$ mol CO_2 /mol MEA were selected. This lean loading was considered to be similar to values commonly found in experimental and modelling papers regarding plant operations with aqueous MEA, e.g., [Kvamsdal et al. \(2009\)](#). The choice of 5 inner equilibrium stages was somewhat arbitrary, but is justified by the reboiler duties obtained through our modelling approach (see below). An increase in the number of equilibrium stages would merely slightly reduce the energy duties in the desorber without significantly altering any of the trends observed throughout our simulations.

With the selected lean loading and reboiler temperature, the model has returned a total pressure of $p = 188$ kPa. [Fig. 3](#) shows some results for the desorber modelling without the addition of co-solvent. The vapor phase concentration profiles for the specific case in which the temperature of the condenser is fixed at $T_C = 35$ °C are shown in the upper-left corner. With these conditions, CO_2 is produced at a purity of about 97%. In the upper-right corner of [Fig. 3](#), one can see how increasing the temperature of the condenser allows more water to be drawn out as a product, diluting the CO_2 stream. Higher condenser temperatures imply lower reflux ratios (bottom-left corner) and lower condenser duties (bottom-right corner). Boil-up ratios and reboiler duties are also reduced with increasing condenser temperatures, but very slightly.

The reboiler duties evaluated for this process ($Q_R \approx 3.5$ MJ/kg CO_2) are very similar to those obtained in real industrial CO_2 capture applications before process modifications such as vapor recompression and advanced flash stripping ([Rochelle, 2016](#)). This suggests that our modelling approach, though highly simplified, is sophisticated enough to deliver credible data on the design and operation of CO_2 desorber columns.

3. Results and discussion

3.1. Co-solvent candidates

For evaluating a series of co-solvent candidates, one needs a good database of Antoine parameters. For an initial assessment, the database compiled by [Yaws and Satyro \(2015a\)](#) showed to be a very good resource, with more than 25,000 organic compounds. However, for the second step of this work, i.e. the desorber simulations, this database proved to be

Table 1 – Organic compounds and the total pressure attained in the reboiler for MEA 30%wt. when $\alpha = 0.2$, $f_{\text{COS}} = 0.1$ and $T = 120$ °C. Case A: co-solvent can be recovered as liquid at 25 °C and 101.325 kPa.

Name	CAS	p/kPa
2,3-butadien-1-ol	18913-31-0	959.6
Vinyl formate	692-45-5	753.9
Hydrogen cyanide	74-90-8	396.8
3-methoxy-1-propene	627-40-7	394.8
1,trans-2-dimethylcyclopropane	2402-06-4	374.3
Dimethylacetylene	503-17-3	369.3
Divinyl ether	109-93-3	357.9
3-methyl-1-butene	598-23-2	350.5
(S)-(-)-propylene oxide	16088-62-3	347.7
1,cis-2-dimethylcyclopropane	930-18-7	343.7

Table 2 – Organic compounds and the total pressure attained in the reboiler for MEA 30%wt. when $\alpha = 0.2$, $f_{\text{COS}} = 0.1$ and $T = 120$ °C. Case B: co-solvent can be recovered as liquid at 25 °C and 1013.25 kPa.

Name	CAS	p/kPa
Propane	74-98-6	1082.1
Vinyl alcohol	557-75-5	1057.2
Cyclopropane	75-19-4	1013.8
Cyanogen	460-19-5	969.3
Methylacetylene	74-99-7	962.2
2,3-butadien-1-ol	18913-31-0	959.6
Allene	463-49-0	866.2
Dimethyl ether	115-10-6	847.3
Methylamine	74-89-5	764.7
Vinyl formate	692-45-5	753.9

unsuitable. This is because one needs heat capacity data to calculate the energy balances inside a desorber column, and heat capacity data for many of the compounds compiled by [Yaws and Satyro \(2015a\)](#) is quite difficult to be found. Therefore, for the second part of this study, the data compiled by [Yaws \(2003\)](#) has been used instead. Though displaying a smaller dataset, coming slightly short of 5000 organic compounds, this second resource compiles both Antoine parameters and heat capacity parameters for roughly the same array of chemicals.

At any rate, employing the database of [Yaws and Satyro \(2015a\)](#), one can employ the shortcut calculation described previously in Section 2.2 to estimate the total pressure of the reboiler. For the present calculations, we are assuming that the lean amine should be recovered at $\alpha = 0.2$ mol CO_2 /mol MEA and 120 °C. We have also fixed $f_{\text{COS}} = 0.1$ mol co-solvent/mol water for the sake of simplicity, though one should notice that the reboiler pressure will asymptotically approach the saturation pressure of the pure co-solvent as f_{COS} becomes larger. Finally, we have separated our analysis in two cases. In Case A, the co-solvent can be recovered as a liquid at 25 °C and 101.325 kPa, meaning the co-solvent can be ordinarily recovered by cooling. In Case B, the co-solvent can be recovered as a liquid at 25 °C and 1013.25 kPa, meaning the co-solvent can be recovered after cooling and compression.

The total pressures obtained by following these two analyses have been ranked in descending order and the results are shown in [Table 1](#) and [Table 2](#). We took the liberty of manually removing from the list all compounds that presented halogens (F, Cl, Br, I), phosphorus, selenium, silicon and any heteroatoms other than oxygen and nitrogen. This has been done to prevent clear cases in which the co-solvent would potentially accelerate the degradation of the amine ([Mosser et al.,](#)

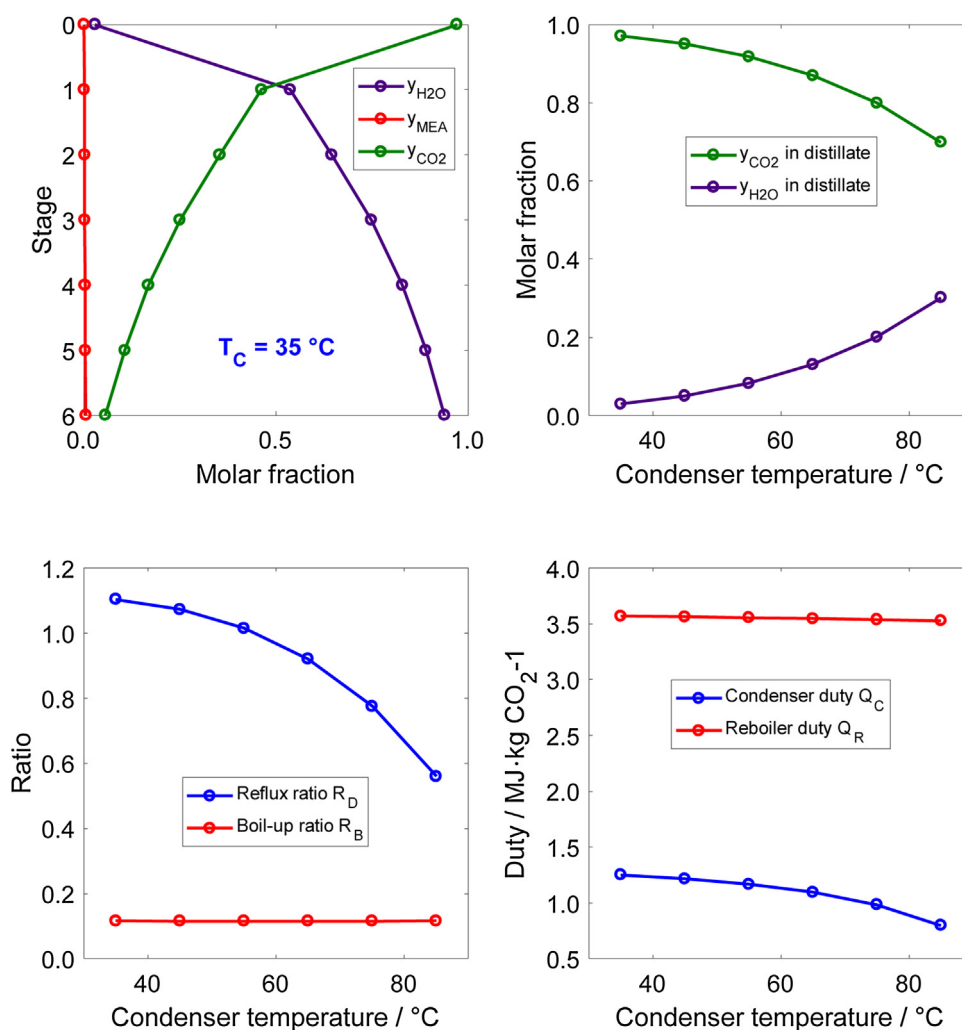


Fig. 3 – Desorber modelling without co-solvent. Vapor phase concentration profiles for case in which the condenser temperature is $35^\circ C$, then distillate concentrations, reflux and reboiler ratios and condenser and reboiler duties as functions of condenser temperature.

2011, 2019). That brings a meaningful trimming of options, as the vast majority of ranked co-solvents are chemicals such as methyl 1,1,2,2-tetrafluoroethyl ether, fluorocarbonyl isocyanate and borane dimethylsulfide. By eliminating these candidates, the list is vastly reduced.

Other clearly harmful chemicals have been deliberately left in Table 1 and Table 2 for illustration purposes. For example, no one would recommend using hydrogen cyanide (used as chemical weapon in the First World War) or cyanogen as co-solvents due to their high toxicity. Similarly, the presence of methylamine in Table 2 should raise the concern of whether this co-solvent would really act as an inert gas – quite probably, it would react with CO_2 (Hajmalek et al., 2013). Therefore, the use of the shortcut method for evaluating co-solvents requires judgement. And if this applies to obvious harmful chemicals such as hydrogen cyanide, it also applies to every other chemical which might be unfamiliar to the reader. The compilation and understanding of material safety datasheets (MSDS) of each component is essential for evaluating possible co-solvents.

The Appendix A of this work includes an expanded version of Table 1 and Table 2 including chemical structures and hazard symbols for every co-solvent candidate. What can be summarized from a cursory study of the MSDS is that all of the prospective organic co-solvents found through this

methodology are flammable. This is perhaps not surprising. One must notice, however, that some of them are extremely unstable. For example, neither cyclopropane nor vinyl alcohol can be obtained commercially due to their high instability, with the former quickly combusting in the presence of oxygen and the latter being spontaneously converted to acetaldehyde within a short period of time after production. Ethylene oxide (which should deliver 456.3 kPa of total pressure following our methodology) is so unstable that one handbook states that “Although soluble in water, solutions will continue to burn until diluted to approximately 22 volumes of water to one volume of ethylene oxide” (Pohanish, 2012). This begs for caution and discernment when considering to apply any of the co-solvents proposed in this study in real life applications, whether in industrial or laboratory scale levels.

Together with the MSDS, one should carefully consider the chances of the co-solvent reacting with CO_2 or with the amine, since both possibilities would have harmful effects on the desorption process. In our previous work, we have briefly discussed the reactivity of MEA with different organic solvents (Wanderley et al., 2020). These general rules do not preclude the necessity of empirical data and experimental investigation. Everything obtained through shortcut methods and mathematical modelling needs to be validated by scientific observation.

What would happen if the co-solvent is not entirely miscible with the aqueous amine? In that case, a second liquid phase would be formed containing a proportionally high concentration of the co-solvent. This second liquid phase still has to be in equilibrium with the vapor phase, and the partial pressure of the co-solvent will end up being actually larger than it would appear to be through the application of a single-liquid phase calculation. Additionally, an immiscible co-solvent would probably facilitate the recovery of this compound from the liquid lean amine product, more easily closing the co-solvent loop around the desorber. Therefore, the immiscibility of the co-solvent might actually be beneficial to the process. Conversely, if the co-solvent is miscible and *does* affect the chemical equilibrium between CO₂ and the amine, the current understanding of VLE behavior in water-lean solvents implies that this co-solvent will help desorb the CO₂ by shifting the reaction towards less carbamate formation (Wanderley et al., 2019, 2020; Yuan and Rochelle, 2018, 2019). The net effect on the CO₂ stripping process would, therefore, also be positive. At any rate, the concerns raised at the end of Section 2.1 show that our methodology is actually *pessimistic* towards the use of volatile co-solvents, and thus that the results obtained with our simulations are generally quite conservative.

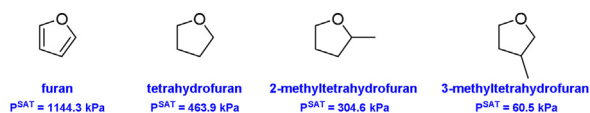


Fig. 4 – Series of furans and their saturation pressures at 120 °C, calculated with the Antoine parameters from Yaws (2003).

3.2. Desorber with series of furan derivatives

To exemplify the effects of adding a volatile co-solvent to the desorber, we introduce the following series of furans shown in Fig. 4. This series is presented in a descending order of volatility, with furan being the most volatile co-solvent and 3-methyltetrahydrofuran being the least. The saturation pressures of these components at 120 °C have been calculated with the Antoine parameters provided in Yaws (2003) and are printed on Fig. 4. Conversely, their boiling points at 101.325 kPa are calculated by the same approach as being 31.3 °C for furan, 64.8 °C for tetrahydrofuran, 80.2 °C for 2-methyltetrahydrofuran and 138.0 °C for 3-methyltetrahydrofuran. In other words, 3-methyltetrahydrofuran seems to be less volatile than water according to the parameters provided by Yaws (2003). We

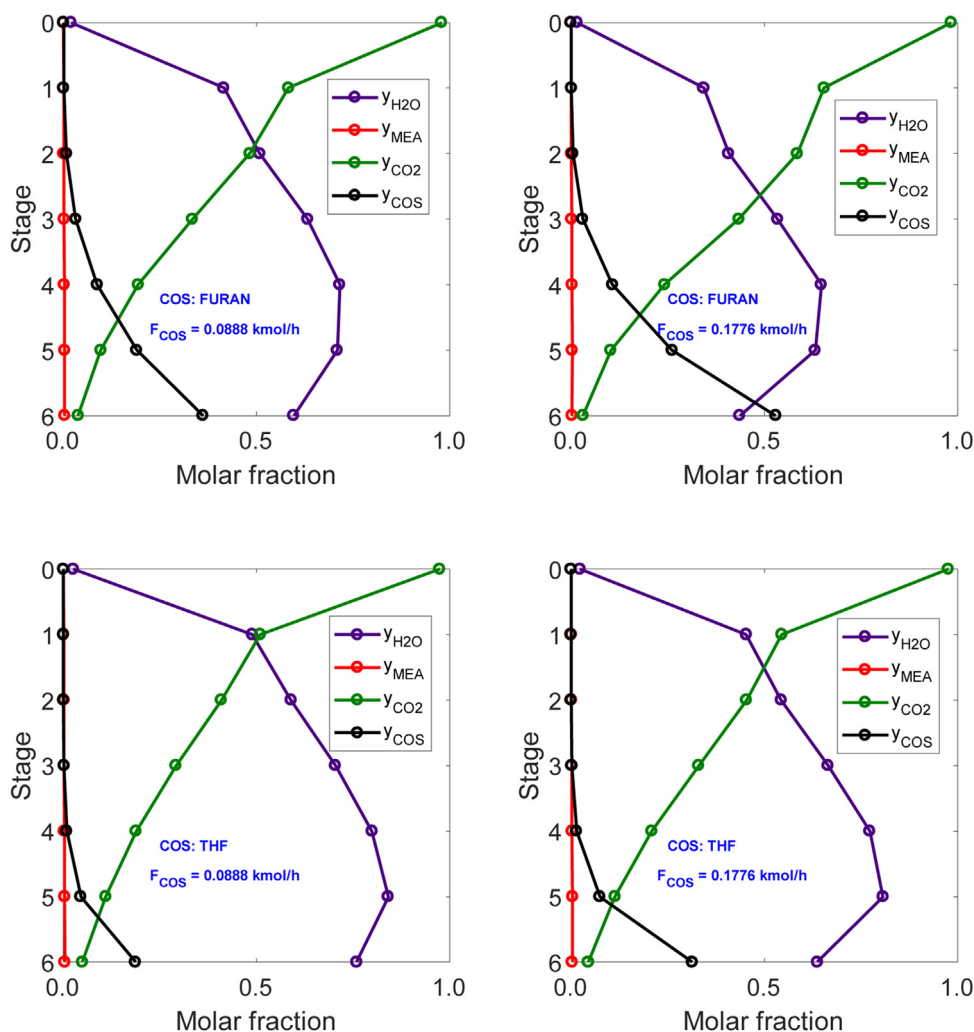


Fig. 5 – Vapor phase molar fractions of water, amine, CO₂ and co-solvent in a desorber with furan and tetrahydrofuran injection. Desorber with 5 + 2 equilibrium stages. The rich solvent molar flow rate is 1 kmol/h. Rich loading $\alpha = 0.5$, lean loading $\alpha = 0.2$, temperature at the reboiler of 120 °C and temperature at the condenser of 35 °C. The co-solvent molar flow rates are printed on the graphs.

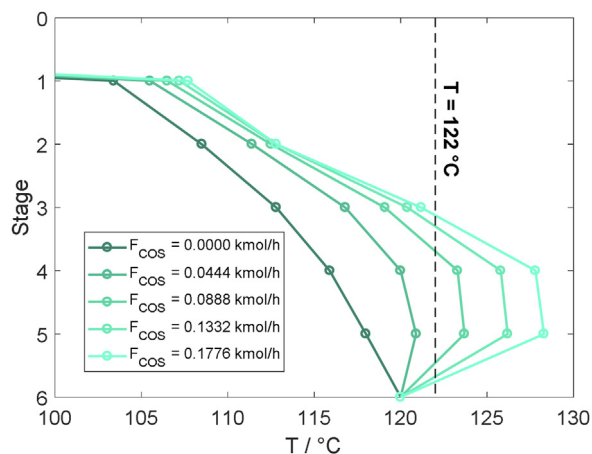


Fig. 6 – Temperature profiles with furan as co-solvent. Desorber with 5 + 2 equilibrium stages. The rich solvent molar flow rate is 1 kmol/h. Rich loading $\alpha = 0.5$, lean loading $\alpha = 0.2$, temperature at the reboiler of 120 °C and temperature at the condenser of 35 °C.

must highlight that the later version of this databook provides drastically different parameters for 3-methyltetrahydrofuran (Yaws and Satyro, 2015a), and that this solvent might as well be more volatile than water. Nevertheless, the series as it is shown is deemed to be illustrative of the effects of decreasing volatilities of possible co-solvents.

The vapor phase molar fraction profiles of water, MEA, CO₂ and co-solvent are shown for the addition of furan and tetrahydrofuran at different flow rates in Fig. 5. A few things might stand out in this image. The first one is that, for these two candidates, the co-solvent can be found concentrated in bulk at the bottom of the desorber, i.e. the co-solvent does not permeate all the way up to the distillate. This happens even though furan has a boiling point below 35 °C, which is the temperature of the condenser. The reason is that the co-solvent is effectively being washed away by the rich amine fed to the top of the desorber, condensing into the liquid phase as it flows upwards.

The second thing that can be noticed on Fig. 5 has to do precisely with the condensation of the co-solvent. This is well evidenced by looking at the concentration profile of water in the column (purple lines), specially for higher co-solvent flow rates. The water molar fraction in the last stage of the desorber ($S = 5$) is higher than that in the reboiler ($S = 6$), which can be graphically perceived as a *bulge* in $S = 5$. This is because the co-solvent is being injected as vapor to the reboiler and initiating its condensation precisely at the stage directly above it. Condensation is an exothermic process. As a result, the last stage of the desorber becomes warmer than the reboiler itself, which leads to increased water vaporization and a bulge in its concentration profile. This is further illustrated in Fig. 6, which shows the temperature profiles in the desorber when using furan as a co-solvent. (Notice that the point referring to the stage $S = 0$ is not shown, but that we have already specified that the temperature in the condenser is $T = 35$ °C.)

The condensation of co-solvent and subsequent formation of a temperature bulge can be seen as potentially beneficial to the process, since it seemingly induces a reduction of the heat duty demands that must be supplied directly to the reboiler. However, this impression is misleading. Firstly, the temperature bulge might defeat the purpose of the addition of a volatile co-solvent, which is to keep the temperatures in the column

below a threshold of 120 °C to prevent amine degradation. For example, the addition of $F_{\text{COS}} > 0.1776$ kmol/h of furan to the reboiler might possibilitate the recovery of CO₂ at about 340 kPa while keeping the reboiler temperature at 120 °C, but the stage right above the reboiler will reach increasingly higher temperatures, which creates a clear barrier to how much co-solvent can be added. Secondly, one cannot ignore the energy required for separating, heating up and vaporizing the co-solvent stream when calculating the total reboiler duties. For this reason, instead of presenting the reboiler duties simply as the heat required by the reboiler alone, we have decided to add to this value the energy required to heat up a liquid co-solvent stream from 25 °C up to 120 °C and to vaporize it. This is a conservative approach. Even if the liquid co-solvent is not recovered at 25 °C but at a higher temperature, one must remember that this co-solvent has to be separated by an unitary process such as through the use of a second distillation column, which will effectively probably consume more energy than the sensible heat + vaporization heat that is being considered in the current approach.

$$Q = Q_R + Q_{\text{COS}} = Q_R + \left(\int_{25^\circ\text{C}}^{120^\circ\text{C}} C_{p,\text{COS}} \cdot dT + \Delta H_{\text{COS}}^{\text{vap}} \right) \cdot \frac{F_{\text{COS}}}{D \cdot y_{\text{CO}_2}} \quad (12)$$

Fig. 7 shows some other features of the process operating with a series of furan as co-solvents. On the upper-left corner, one can see how increasing co-solvent flow rates allow for increasing operational pressures, which are higher for the more volatile co-solvents. While furan possibilitates the recovery of CO₂ at a maximum of 230 kPa, tetrahydrofuran sets the limit at 225 kPa and so forth. These limiting conditions are denoted by the stars in Fig. 7, which mark the highest F_{COS} for each co-solvent before the estimated temperatures at any stage of the desorber surpass 122 °C. The least volatile co-solvent, 3-methyltetrahydrofuran, actively demands that the pressure of the desorber is decreased so as to keep the reboiler temperature at 120 °C. On the upper-right corner, one can see that all co-solvents induce an increase in energy requirements following the approach outlined in the previous paragraph. These shifting energy requirements can be correlated to the changes in reflux ratios and boil-up ratios seen on the bottom-left corner of Fig. 7. By promoting an overall increase in desorber pressures while failing to reach upwards to the distillate, the addition of this series of furans essentially acts on the vaporization of water itself. Volatile co-solvents such as furan increase the pressure of the desorber so that less water is condensed in the distillate, which means lower reflux ratios. Conversely, boil-up ratios must increase to account for the circulation of this new addition to the column. On the other hand, a non-volatile co-solvent such as 3-methyltetrahydrofuran allows for more condensation of water through reduction of the operational pressure of the process, increasing the reflux ratios and decreasing boil-up ratios. Coupled with the heat required for providing this vaporized co-solvent stream, the net result of these effects is what is observed on the upper-right corner of Fig. 7. Finally, the bottom-right corner of Fig. 7 shows the molar fractions of co-solvents in the distillate and in the bottom product. As mentioned previously, the co-solvents in the series of furans essentially do not reach the distillate, meaning $y_{\text{COS}} \approx 0$ for the whole set of simulations regardless of solvent flowrates.

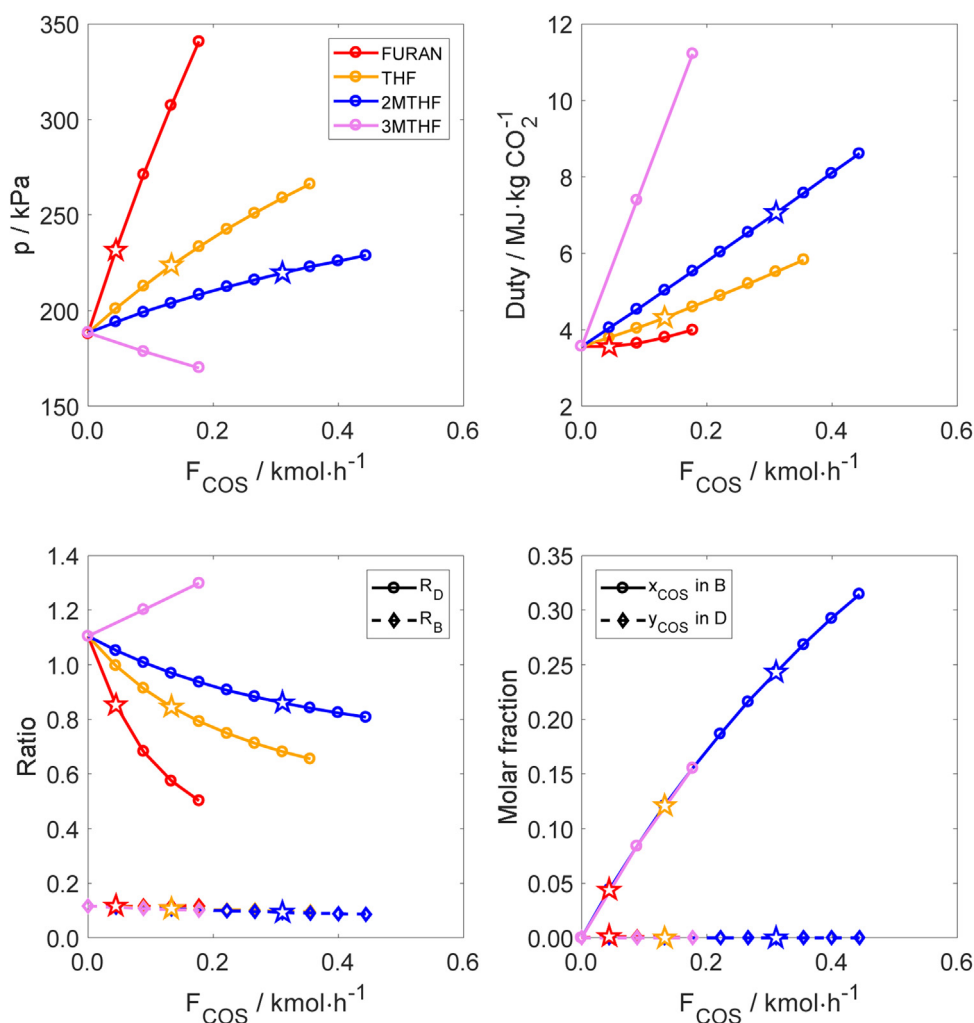


Fig. 7 – Results for simulations with series of furans as co-solvents: pressure of the column, total heat duties, reflux ratio and boil-up ratio, co-solvent concentrations in the product streams. Desorber with 5 + 2 equilibrium stages. The rich solvent molar flow rate is 1 kmol/h. Rich loading $\alpha = 0.5$, lean loading $\alpha = 0.2$, temperature at the reboiler of 120 °C and temperature at the condenser of 35 °C. The stars mark the highest evaluated value of F_{COS} before the temperature at any stage of the column reaches 122 °C.

As a result, the bulk of co-solvent added to the desorber comes out of the column mixed with the lean amine stream, thus requiring a single separation process afterwards.

Finally, we must mention that, though the temperature of the condenser for all of our simulations has been kept at $T_C = 35$ °C, the Appendix A of this study provides an analysis of the effects of varying this parameter. Our results show that, when identifying the overall behavior of the high-pressure desorption process, varying T_C is not of highest priority and can be ignored for the sake of simplicity.

The takeaways from this exercise with a series of furans as co-solvents are:

- 1 The solvents from this series are not volatile enough to percolate the desorber all the way up to the distillate (Fig. 5 and Fig. 7), even though the boiling point of furan itself is calculated at 31.3 °C with the parameters from Yaws (2003). Therefore, the way that the co-solvents of this series affect desorber pressures is by accumulating at the bottom stages of the column without coming out at the top.
- 2 The increased desorber pressures inhibit water vaporization (Fig. 5).
- 3 Since these co-solvents do not reach the distillate and act by depressing the vaporization of water, the temperatures

achieved in the column must be overall higher than in the absence of co-solvents (Fig. 6). These temperatures increase due to (i) the co-solvent stream exothermically condensing in the column and (ii) the water being unable to endothermically evaporate. If there was no increase in temperatures in the desorber, it is doubtful that CO_2 would be sufficiently stripped: the driving force to desorb CO_2 must be provided by something else now that less water is being vaporized and no co-solvent is coming to the upper stages. This something else is heat.

- 4 Eventually, the addition of co-solvent forms a temperature bulk large enough so that the whole purpose of avoiding solvent degradation is defeated (Fig. 6). Therefore, there is a cap to how much co-solvent of this kind can be added, and of how much increase in pressure can be attained by this methodology.
- 5 As the co-solvent comes out of the column mixed with the lean amine (Fig. 7), a new separation step is required to remove the co-solvent from the bottom stream and keep it in a closed loop around the reboiler.

Overall, addition of a co-solvent typified by the series of furans does not seem to be a good idea for attaining higher CO_2 delivery pressures. The fact that no co-solvent reaches

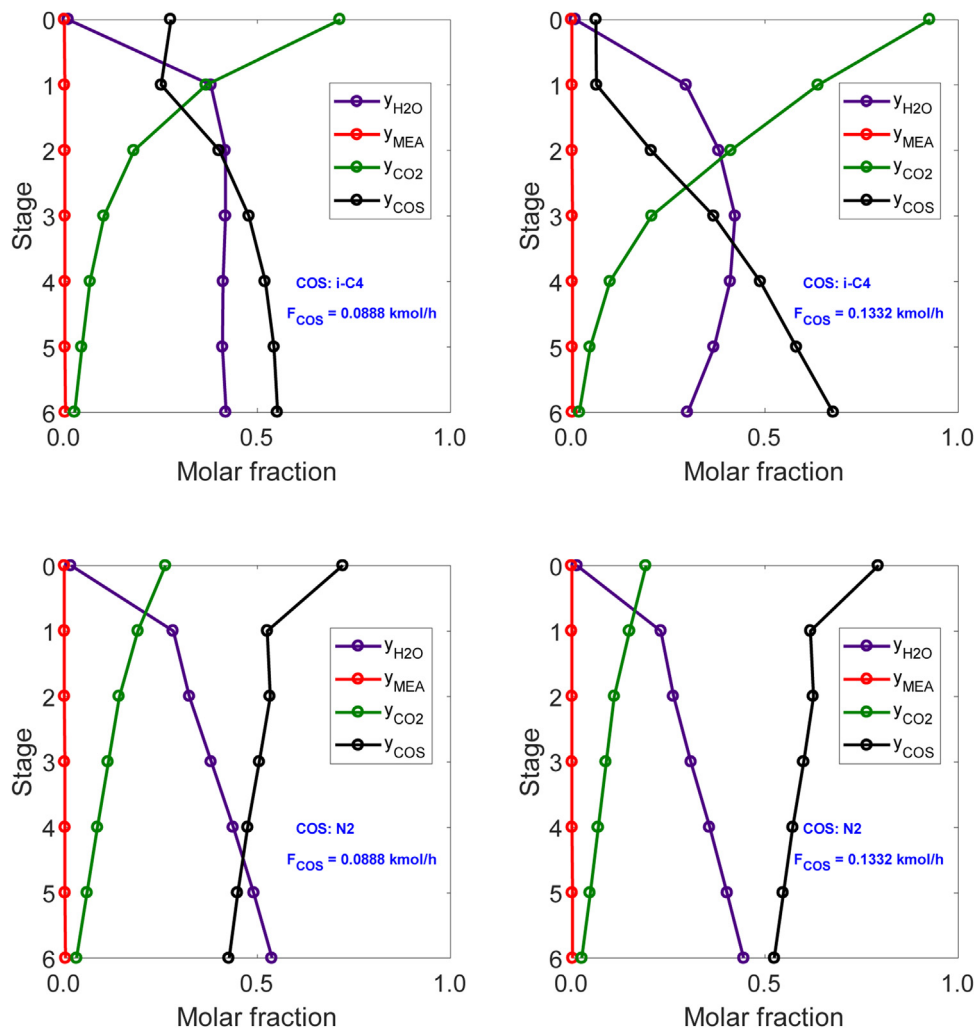


Fig. 8 – Vapor phase molar fractions of water, amine, CO₂ and co-solvent in a desorber with isobutane and nitrogen injection. Desorber with 5 + 2 equilibrium stages. The rich solvent molar flow rate is 1 kmol/h. Rich loading $\alpha = 0.5$, lean loading $\alpha = 0.2$, temperature at the reboiler of 120 °C and temperature at the condenser of 35 °C. The co-solvent molar flow rates are printed on the graphs.

the distillate imply a strict cap on how much pressure can be gained by this methodology. With this in mind, let us consider the case for employing hyper volatile co-solvents.

3.3. Desorber with hyper volatile co-solvents

By *hyper volatile co-solvents*, we mean co-solvents that are not liquids at 25 °C and 101.325 kPa. To be more precise, in this section we will consider the cases of dimethyl ether and isobutane, whose boiling points are respectively -24.8 °C and -11.7 °C following the Antoine parameters of *Yaws (2003)*. Additionally, pure nitrogen has been modelled as a co-solvent and its performance is presented in this section as well. Using the Antoine parameters provided by *Yaws and Satyro (2015b)*, the boiling point of nitrogen is -195.8 °C. This means that nitrogen cannot be separated from CO₂ by condensation, but rather that CO₂ itself must be condensed out of the distillate in case this co-solvent is employed. In other words, nitrogen is not a practical co-solvent, and its presence in this section is merely for illustration purposes as an example of a compound with very high volatility.

Fig. 8 is very similar to *Fig. 5*, showing the vapor phase molar fractions of each component for a desorber operating with isobutane and with nitrogen as co-solvents injected at distinct molar flow rates. This time, however, one can clearly see

that the co-solvent percolates the whole column and comes out at the distillate. Also, differently from in the previous analysis, the water concentration bulge in $S = 5$ has disappeared. Results for the injection of dimethyl ether are not shown in *Fig. 8* due to space limitations, and also due to the fact that the curves observed with this particular co-solvent follow a trend in between those obtained by injection of isobutane and by injection of nitrogen.

Fig. 9 shows the temperature profiles in the desorber brought by the addition of dimethyl ether as co-solvent. As suggested in the discussion of *Fig. 8*, the temperature bulge caused by the addition of compounds in the series of furans does not immediately appear when employing hyper volatile co-solvents. Indeed, it is seen that the addition of a small F_{COS} of dimethyl ether provokes a decrease in temperature at the bottom of the column and an increase at the top. Since the condensation of co-solvent is no longer constrained to the bottom stages, the temperatures in the desorber become more evenly distributed. This is not to say that a situation will not arise wherein a temperature bulge can be noticed – it just might happen at high co-solvent molar flow rates. Before that, a very noticeable increase in the operational pressures of the desorber can be verified with the addition of hyper volatile co-solvents.

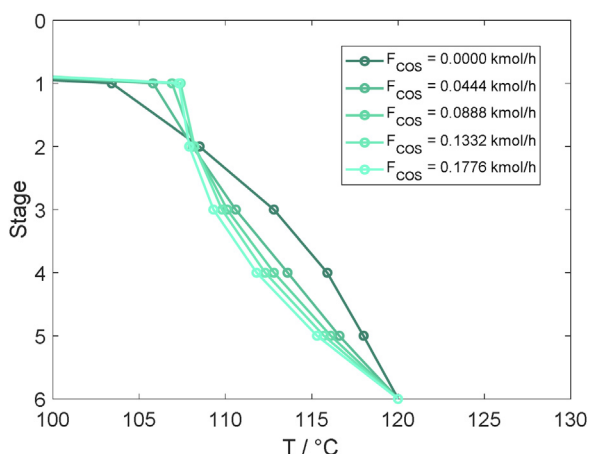


Fig. 9 – Temperature profiles with dimethyl ether as co-solvent. Desorber with 5 + 2 equilibrium stages. The rich solvent molar flow rate is 1 kmol/h. Rich loading $\alpha = 0.5$, lean loading $\alpha = 0.2$, temperature at the reboiler of 120 °C and temperature at the condenser of 35 °C.

Fig. 10 shows the same set of features previously discussed in Fig. 7, though the results are now more counter-intuitive. Consider for example the plot in the upper-left corner of Fig. 10. The pressures achieved by the addition of hyper volatile

co-solvents are clearly higher than those attained by the series of furans, reaching 500 kPa with a comparatively small injection of dimethyl ether. However, this time the higher pressures are provided by the least volatile co-solvents: nitrogen is more volatile than dimethyl ether, which is more volatile than isobutane, and yet it is isobutane the co-solvent that is able to pressurize the desorber the most. The key to understanding this can be found in the bottom-left corner of Fig. 10. The huge majority of the nitrogen injected into the desorber streams upwards and leaves together with the distillate, and thus the reflux ratio decreases steeply for higher flow rates of nitrogen. For dimethyl ether and isobutane, the reflux ratios are a bit larger, meaning that a parcel of the co-solvents is being condensed at the top of the column and being allowed to recirculate. This recirculation causes the concentrations of co-solvent in both liquid and vapor phases to build up more than they would otherwise. It is this build up that allows for higher pressures to be achieved with isobutane than with nitrogen.

In the bottom-right corner of Fig. 10, one can see that the amount of dimethyl ether and isobutane leaving at the bottom fraction of the desorber together with the lean amine is not negligible at all, whereas that of nitrogen approaches 0.2% at best. In fact, in the case of isobutane, the condensation of the co-solvent becomes so relevant that an inflection in the molar fraction obtained in the distillate is observed

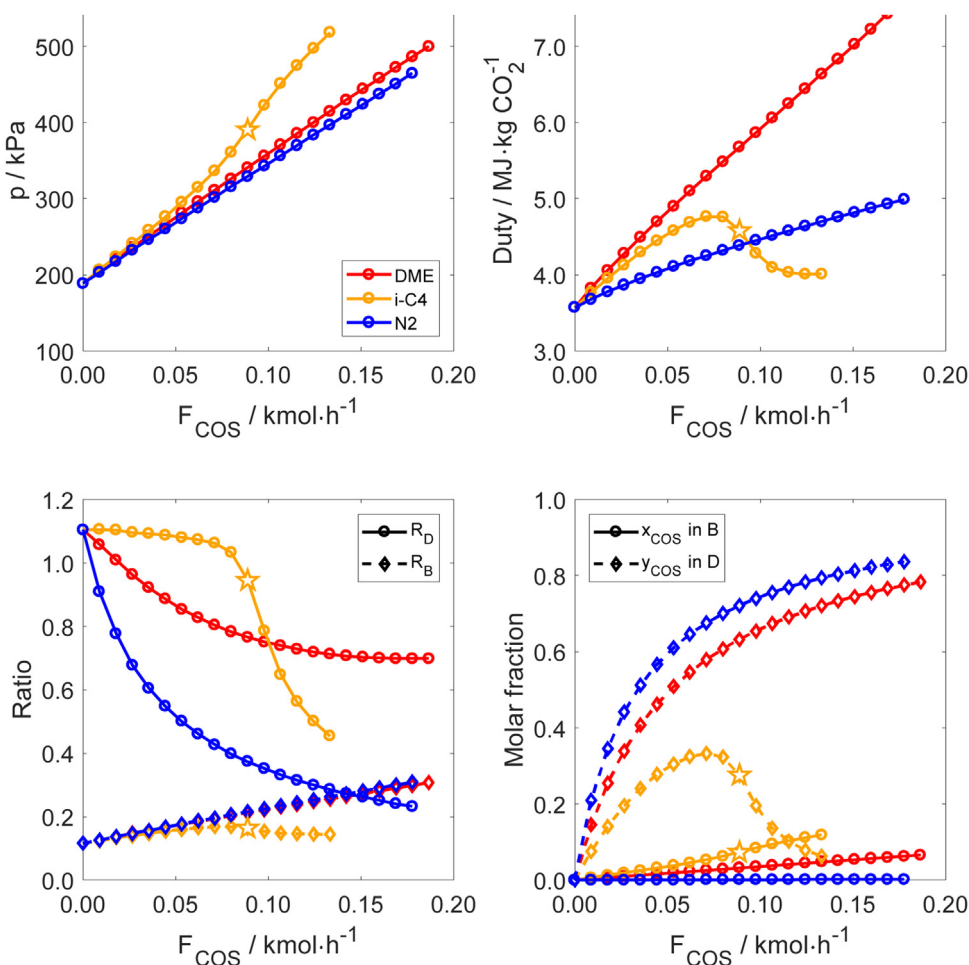


Fig. 10 – Results for simulations with hyper volatile co-solvents: pressure of the column, total heat duties, reflux ratio and boil-up ratio, co-solvent concentrations in the product streams. Desorber with 5 + 2 equilibrium stages. The rich solvent molar flow rate is 1 kmol/h. Rich loading $\alpha = 0.5$, lean loading $\alpha = 0.2$, temperature at the reboiler of 120 °C and temperature at the condenser of 35 °C. The stars mark the highest evaluated value of F_{COS} before the temperature at any stage of the column reaches 122 °C.

for increasingly high F_{COS} (and increasingly high pressures). At high co-solvent flow rates F_{COS} , isobutane behaves much like one of the furan derivatives analyzed in Section 3.2: the co-solvent barely reaches the top of the column, and both the reflux ratio R_D and the co-solvent concentration in the distillate y_{COS} fall steeply. Simultaneously, the formation of a bulk of isobutane at the bottom of the desorber creates a clear threshold at $F_{\text{COS}} = 0.0888 \text{ kmol kmol/h}$ and $p = 390 \text{ kPa}$, above which the temperatures in the upper stages of the column rise above $122 \text{ }^\circ\text{C}$. This has not been observed either for dimethyl ether or for nitrogen, and thus only the curves referring to isobutane are marked with a star in Fig. 10. Interestingly, thus, though the addition of isobutane delivers a fast increase in desorption pressures with comparatively low co-solvent flow rates, this increase is capped at $p = 390 \text{ kPa}$, whereas no such cap is observed for dimethyl ether or for nitrogen.

Overall, hyper volatile co-solvents appear to be more promising than the chemicals exemplified by the series of furans. Since the co-solvent percolates all the way up to the distillate, there is enough driving force to desorb CO_2 even without large shifts in temperature. Recirculation of the co-solvent throughout the whole column allows for higher pressures to be achieved for smaller flow rates of additive. Finally, though some co-solvent leaves the column mixed with the lean amine, its bulk can be found in the vapor distillate together with CO_2 . Recovery of the co-solvent can be performed by pressurization and cooling of the distillate or directly through chilling, depending on the difference of boiling points of vapor products. The boiling point of CO_2 is $-78.5 \text{ }^\circ\text{C}$ at 101.325 kPa according to the parameters of Yaws and Satyro (2015a), thus quite far from the boiling points of dimethyl ether and isobutane.

However, we must keep in mind that one of the objectives of this approach is to reduce the compression duties of the CO_2 capture plant. Let us consider the example of high-pressure desorption with dimethyl ether. On the upper-left corner of Fig. 10, one sees that the distillate stream can be produced at around 500 kPa when 0.185 kmol/h of dimethyl ether is injected into the reboiler. This is a 165% increase from the delivery pressure obtained without the addition of the co-solvent. At the same time, a parcel of the dimethyl ether will come out with the distillate. In the aforementioned example, the molar flow rate of vapor product is 360% higher than that when not employing the co-solvent. The method to recover the dimethyl ether in the CO_2 stream will depend on the availabilities at the CO_2 capture plant location. If there are cold streams that can be used, perhaps chilling is a proper alternative for dimethyl ether condensation. Otherwise, cooling and compression might be a better solution. To discuss these two alternatives, we have employed the Antoine parameters of CO_2 obtained in Yaws (2003) to perform flash calculations on the vent product of the desorber.

To continue on the example of high-pressure desorption with dimethyl ether as a co-solvent delivering CO_2 at 500 kPa : the distillate comes out with 21.1% CO_2 , 78.3% dimethyl ether and 0.6% water at $35 \text{ }^\circ\text{C}$. If one chooses to simply compress and cool down this product in a compression train, keeping the temperature at $35 \text{ }^\circ\text{C}$, one will see that at 1000 kPa there is still 55.5% dimethyl ether in the vapor stream, then at 1500 kPa this value is reduced to 33.7%, then at 2000 kPa the dimethyl ether concentration is 22.7% and so on. It is only at around 5900 kPa and $35 \text{ }^\circ\text{C}$ that the dimethyl ether con-

centration in the vapor stream falls below 1%, and that of CO_2 consequentially reaches above 99%. What this means is that, although the Δp of compression will be reduced with the use of dimethyl ether, the amount of gas being compressed is increased since now it encompasses the dimethyl ether as well. Depending on the conditions of the CO_2 capture plant, chilling the product could be more appropriate. Keeping a constant pressure of 500 kPa , the dimethyl ether concentration in the vapor falls to 49.5% at $0 \text{ }^\circ\text{C}$, then to 32.2% at $-10 \text{ }^\circ\text{C}$ and so forth, finally reaching below 1% at $-53 \text{ }^\circ\text{C}$. Otherwise, one could consider a combination of chilling and pressurization: at 1000 kPa the dimethyl ether concentration in the vapor product reaches below 1% at $-36 \text{ }^\circ\text{C}$, and at 1500 kPa it is at $-24 \text{ }^\circ\text{C}$. We will refrain from going in too deep with regards to dimethyl ether recovery alternatives, but we would like to stress out that these considerations should be taken into account before assertively stating whether high-pressure desorption with the injection of co-solvents is feasible or not.

To summarize the results of this exercise on hyper volatile co-solvents:

- 1 Hyper volatile co-solvents (solvents that are gaseous at $25 \text{ }^\circ\text{C}$ and 101.325 kPa) can deliver higher pressures than regular co-solvents such as those of the furan series, inasmuch as they are able to percolate the whole desorber and reach the distillate (Fig. 8 and Fig. 10).
- 2 With hyper volatile co-solvents, the recirculation of the solvent inside the column is a factor that strongly impacts the pressures reached in the desorber. With that in mind, a very volatile co-solvent might be worse than a less volatile solvent, since the latter can be easily recirculated while the former might just leave the desorber in the distillate (which, of course, depends on how the condenser is designed) (Fig. 8 and Fig. 10).
- 3 As the condensation of co-solvent is a lesser issue with hyper volatile co-solvents, temperature bulges are largely avoided. Simultaneously, the fact that the co-solvent reaches the distillate means it provides driving forces for the stripping of CO_2 . This raises the threshold for how much co-solvent can be added to the column, and of how much pressure can be gained with this addition (Fig. 9). Isobutane is a fine example of a co-solvent that lies in the threshold between hyper-volatile co-solvents and those represented by the series of furans, behaving like either of them depending on the operational conditions of the desorber.
- 4 The hyper volatile co-solvent most likely leaves the column both in the distillate as in the bottom product, but mainly in the distillate. This co-solvent in the distillate can be recovered with compression and cooling or with chilling. A specific case-by-case analysis must be performed to find which alternative, if any, enables the use of high-pressure desorption. The co-solvent in the bottom product must be recovered with a secondary separation process.

The last point is perhaps one of the most important conclusions of this work. If it is true that higher pressures are achieved when the co-solvent is allowed to reach the distillate but also condenses and recirculate inside the desorber, then it is inevitable that a proper co-solvent for high-pressure desorption will come out fractionated between the vapor and liquid products of the stripper. Then one will require two extra separation steps, not merely one, in order to recover the co-solvent.

4. Conclusion

High-pressure desorption has been evaluated as an alternative for producing CO₂ at higher pressures whilst keeping the maximum solvent temperature below 120 °C, thus avoiding amine degradation. A shortcut methodology has been developed to quickly evaluate a series of candidate co-solvents, though this methodology is handicapped by the fact that it ignores the actual conditions of the desorber as a whole (reflux and boil-up ratios, for example). In due course, the modelling and simulation of the stripper has been performed with the injection of a series of co-solvents of low to moderate volatility and then with a series of hyper volatile co-solvents. Low volatile co-solvents such as 2-methyltetrahydrofuran and tetrahydrofuran do not seem to provide pressures high enough to justify their utilization. Simultaneously, their condensation in the desorber possibly creates a temperature bulge that limits how much pressure can be attained through this approach. Alternative hyper volatile co-solvents condense less and percolate the desorber all the way up to the distillate, providing higher pressure gains and avoiding the formation of temperature bulges. This trend is otherwise subverted in the case of nitrogen, which is so volatile that it simply leaves the desorber with little to no recirculation, building comparatively small amounts of pressure. As such, there seems to be a limited volatility range required for the proper design of high-pressure desorption with co-solvents. Nevertheless, this range is defined by the specifications in which the desorber column is operated, specifications which have been proposed in this study only as surrogates for the sake of analyzing trends and identifying patterns.

The use of volatile co-solvent injection as a means for recovering CO₂ at higher pressures seems to be theoretically feasible and a promising alternative process configuration. However, it is also subject to a very careful optimization problem. A suitable co-solvent must make a compromise between being volatile enough to deliver high pressures and not too volatile so that it will still be able to recirculate in the desorber. Additionally, it must have such properties so that it is easily recoverable from both liquid and vapor products without incurring in too many extra operational and capital costs. We are hopeful that the preliminary analysis performed in this work can shed light on the trade-offs inherent to this novel high-pressure desorption process.

Symbol	Units	Meaning
Latin letters		
B	kmol/h	Bottom product
D	kmol/h	Distillate
F	kmol/h	Feed molar flow rate
f_{COS}	mol co-solvent/mol water	Co-solvent fraction
k_1, k_2, k_3	—	Parameters of soft model
L	kmol/h	Liquid molar flow rate
N	—	Number of inner stages of desorber
n_i	mol	Number of mols of i
p	kPa	Total pressure

p_i	kPa	Partial pressure of i
Q	MJ/kg CO ₂	Total regeneration duty
Q _C	MJ/kg CO ₂	Condenser duty
Q _{COS}	MJ/kg CO ₂	Duty for recovery of co-solvent
Q _R	MJ/kg CO ₂	Reboiler duty
R _B	—	Boil-up ratio
R _D	—	Reflux ratio
S	—	Stage of the desorber
T	K	Temperature
V	kmol/h	Vapor molar flow rate
x_i	—	Molar fraction of i in liquid
y_i	—	Molar fraction of i in vapor
Greek letters		
α	mol CO ₂ /mol amine	Loading
ΔH	kJ/mol	Enthalpy of phase change
ν_1, ν_2, ν_3	—	Degrees of advancement
Subscripts		
CO ₂	Referring to CO ₂	
COS	Referring to the volatile co-solvent	
H ₂ O	Referring to water	
MEA	Referring to monoethanolamine	
FEED	Referring to the rich amine feed	
Superscripts		
<i>abs</i>	Referring to absorption	
<i>app</i>	Referring to the amine solvent without CO ₂	
<i>eff</i>	Referring to the amine solvent once reacted with CO ₂	
<i>fresh</i>	Referring to the amine solvent without CO ₂ nor co-solvent	
<i>sat</i>	Referring to saturation	
<i>vap</i>	Referring to vaporization	

Declaration of interests

The authors declare that they have no known competing financial interests or personal relationships that could have appeared to influence the work reported in this paper.

Acknowledgements

This research was funded by the Faculty of Natural Sciences of the Norwegian University of Science and Technology (NTNU).

Appendix A

The Antoine equation for calculating saturation pressures is:

$$\log_{10} \left(\frac{p_i^{\text{sat}}}{0.13332} \right) = A_i - \frac{B_i}{C_i + T - 273.15}$$

Where the temperature T is supplied in K and the saturation pressure p^{sat} is returned in kPa. The coefficients A , B and C for different components are shown in Table A1. The dimensions

Table A1 – Antoine coefficients for the calculation of vapor pressure.

Component	A	B	C	Source
Water	8.05573	1723.6425	233.08	(1)
Monoethanolamine	7.44237	1560.9667	171.200	(2)
Carbon dioxide	7.58828	861.82	271.883	(3)
Furan	7.13277	1145.36	238.023	(3)
Tetrahydrofuran	7.10537	1256.68	232.621	(3)
2-methyltetrahydrofuran	7.13891	1339.48	234.353	(3)
3-methyltetrahydrofuran	6.99166	1430.57	210	(3)
Dimethyl ether	7.19658	984.579	252.976	(3)
Isobutane	6.93388	953.92	247.077	(3)
Nitrogen	6.72531	285.5727	270.09	(1)

Sources: 1 = Yaws and Satyro (2015b), 2 = Yaws and Satyro (2015a), 3 = Yaws (2003).

Table A2 – Polynomial coefficients for the calculation of gas heat capacity.

Component	a	b × 10 ³	c × 10 ⁵	d × 10 ⁹	e × 10 ¹¹
Water	33.174	-3.2464	1.7437	-5.9796	—
Monoethanolamine	33.174	-3.2464	-31.976	158.3	-3.2344
Carbon dioxide	27.437	42.32	-1.9555	3.997	-0.029872
Furan	-13.779	334.89	-22.273	-69.36	-0.81619
Tetrahydrofuran	32.887	24.554	60.226	-623.8	18.528
2-methyltetrahydrofuran	-15.65	607.52	-36.17	79.1	—
3-methyltetrahydrofuran	-15.65	607.52	-36.17	79.1	—
Dimethyl ether	34.668	70.293	16.53	-176.7	4.9313
Isobutane	6.772	341.47	-10.271	-36.85	2.0429
Nitrogen	29.342	-3.5395	1.0076	-4.3116	0.025935

Source: Yaws (2003), except nitrogen, which comes from Coker (2007).

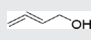

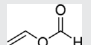
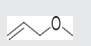




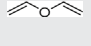
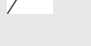

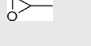

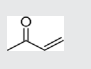

of these coefficients are respectively none (A is adimensional), K and K.

The heat capacity of a single component in the gas phase is given by:

$$C_{p,i} = a_i + b_i \cdot T + c_i \cdot T^2 + d_i \cdot T^3 + e_i \cdot T^4$$

Where the temperature T is supplied in K and the heat capacity C_p is returned in J/mol·K. The polynomial coefficients a, b, c, d and e for different components are shown in Table A2. The dimensions of these polynomial coefficients are respectively J/mol·K, J/mol·K², J/mol·K³, J/mol·K⁴, and J/mol·K⁵.

Table A3 – Organic compounds and the total pressure attained in the reboiler for MEA 30%wt. when $\alpha = 0.2$, $f_{\text{COS}} = 0.1$ and $T = 120^\circ\text{C}$. Case A: co-solvent can be recovered as liquid at 25°C and 101.325 kPa.

Structure	Name	Reboiler pressure/kPa	Hazards
	2,3-butadien-1-ol	959.6	
	Vinyl formate	753.9	could not find information
	3-methoxy-1-propene	394.8	
	1,2-dimethylcyclopropane	374.3/343.7	unstable
	Dimethylacetylene	369.3	
	Divinyl ether	357.9	unstable
	3-methyl-1-butyne	350.5	
	Propylene oxide	347.7/322.6/319.8	
	Methyl vinyl ketone	343.0	

– Table A3 (Continued)

Structure	Name	Reboiler pressure/kPa	Hazards
	Peracetic acid	338.1	
	Ethylcyclopropane	336.4	unstable
	Methyl isopropyl ether	334.7	
	Isopropylamine	334.0	
	Methylethylamine	333.4	
	Furan	333.0	
	Isopentane	330.7	
	1,4-pentadiene	323.2	
	Ethyl vinyl ether	320.8	
	1,3-pentadiene	320.2	
	2-methyl-1-butene	319.3	

The results for the shortcut calculation method of evaluating reboiler pressures are given in Table A3 and Table A4 for two different cases. In Table A3, candidate co-solvents that can be recovered as liquids at 25 °C and 101.325 kPa are given in descending order of volatility. In Table A4, candidate co-

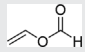





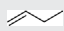

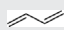

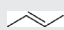

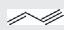


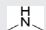

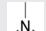

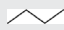



solvents that can be recovered as liquids at 25 °C and 1013.25 kPa are given in descending order of volatility. The hazards of each candidate are shown when found.

Fig. A1 shows the results of the simulation of high-pressure desorption with the injection of different amounts of isobu-

Table A4 – Organic compounds and the total pressure attained in the reboiler for MEA 30%wt. when $\alpha = 0.2$, $f_{\text{COS}} = 0.1$ and $T = 120$ °C. Case B: co-solvent can be recovered as liquid at 25 °C and 1013.25 kPa.

Structure	Name	Reboiler pressure/kPa	Hazards
	Propane	1082.1	
	Vinyl alcohol	1057.2	unstable
	Cyclopropane	1013.8	
	Methyl acetylene	962.2	
	2,3-butadien-1-ol	959.6	
	Allene	866.2	
	Dimethyl ether	847.3	
	Methylamine	764.7	

– Table A4 (Continued)

Structure	Name	Reboiler pressure/kPa	Hazards
	Vinyl formate	753.9	
	Isobutane	598.3	
	Isobutene	571.5	
	1-butene	562.7	
	1,3-butadiene	558.5	
	2-butene	519.3/507.0/485.0	
	Vinylacetylene	518.4	
	Cyclobutene	516.2	could not find information
	Dimethylamine	513.5	
	Trimethylamine	511.2	
	Butane	505.3	
	Ethyl acetylene	488.0	

tane and different condenser temperatures. One can see that the condenser temperature has a very limited influence in the performance of the desorber.

In general, higher condenser temperatures will bring less condensation of the co-solvent, which implies lower reflux ratios R_D , and consequently lower boil-up ratios R_B and lower reboiler duties. There is also a small effect on the concentration of volatile co-solvent in the distillate. Con-

versely, the effects on the concentration of volatile co-solvent in the bottom product and on the pressures that can be attained by co-solvent injection are quite minimal. Overall, there is a repetition in the patterns observed across distinct condenser temperatures. Thus, one can properly evaluate the process by fixing one determined condenser temperature and performing analyses with the remaining variables.

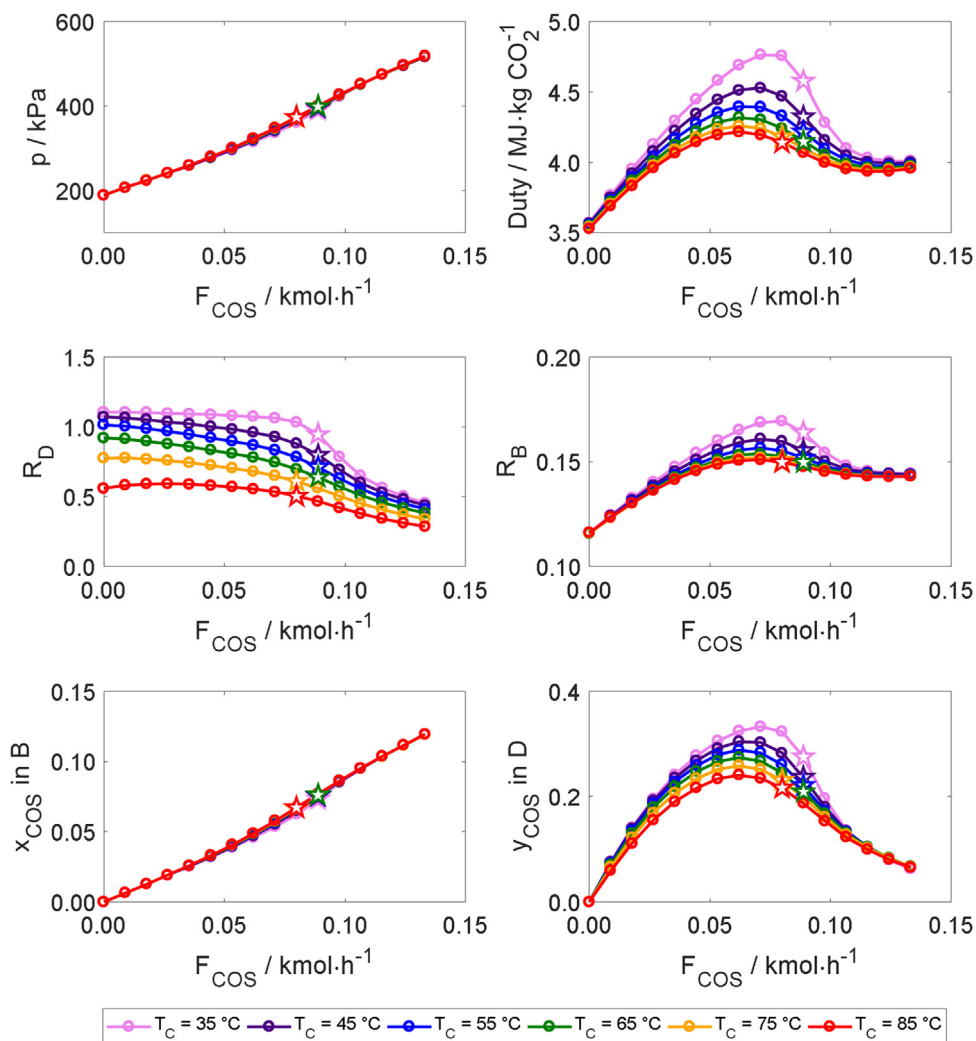


Fig. A1 – Results for simulations with isobutane and different condenser temperatures (T_C): pressure of the column, total heat duties, reflux ratio R_D , boil-up ratio R_B , isobutane concentration in the bottom product (x_{COS}) and isobutane concentration in the distillate (y_{COS}). Desorber with 5 + 2 equilibrium stages. The rich solvent molar flow rate is 1 kmol/h. Rich loading $\alpha = 0.5$, lean loading $\alpha = 0.2$, temperature at the reboiler of 120 °C. The stars mark the highest evaluated value of F_{COS} before the temperature at any stage of the column reaches 122 °C.

References

- Aronu, U.E., Lauritsen, K.G., Grimstvedt, A., Mejdell, T., 2014. Impact of heat stable salts on equilibrium CO₂ absorption. In: Energy Procedia. Elsevier Ltd, pp. 1781–1794, <http://dx.doi.org/10.1016/j.egypro.2014.11.185>.
- Coker, A.K., 2007. Appendix C: physical properties of liquids and gases. In: Ludwig's Applied Process Design for Chemical and Petrochemical Plants. Elsevier, pp. 827–862, <http://dx.doi.org/10.1016/b978-075067766-0/50019-1>.
- Davis, J., Rochelle, G., 2009. Thermal degradation of monoethanolamine at stripper conditions. In: Energy Procedia. Elsevier, pp. 327–333, <http://dx.doi.org/10.1016/j.egypro.2009.01.045>.
- Evjen, S., Wanderley, R., Fiksdahl, A., Knuutila, H.K., 2019. Viscosity, density, and volatility of binary mixtures of imidazole, 2-methylimidazole, 2,4,5-trimethylimidazole, and 1,2,4,5-tetramethylimidazole with water. J. Chem. Eng. Data 64, 507–516, <http://dx.doi.org/10.1021/acs.jced.8b00674>.
- Hajmalek, M., Zare, K., Aghaie, H., 2013. Thermodynamics of CO₂ reaction with methylamine in aqueous solution: a computational study. J. Phys. Theor. Chem. Islam. Azad Univ. Iran 10, 83–89.
- Kim, I., Hoff, K.A., Mejdell, T., 2014. Heat of absorption of CO₂ with aqueous solutions of MEA: new experimental data. Energy Procedia 63, 1446–1455, <http://dx.doi.org/10.1016/j.egypro.2014.11.154>.
- Kriebel, M., 1984. Improved amisol process for gas purification. Energy Prog. (United States) 4, 3.
- Kvamsdal, H.M., Jakobsen, J.P., Hoff, K.A., 2009. Dynamic modeling and simulation of a CO₂ absorber column for post-combustion CO₂ capture. Chem. Eng. Process. Process Intensif. 48, 135–144, <http://dx.doi.org/10.1016/j.cep.2008.03.002>.
- Moser, P., Schmidt, S., Sieder, G., Garcia, H., Stoffregen, T., 2011. Performance of MEA in a long-term test at the post-combustion capture pilot plant in Niederaussem. Int. J. Greenh. Gas Control 5, 620–627, <http://dx.doi.org/10.1016/j.ijggc.2011.05.011>.
- Moser, P., Wiechers, G., Schmidt, S., Elsen, R., Goetheer, E., Khakharia, P., Monteiro, J.G.M.-S., Jens, K.-J., Solli, K.-A., Fernandez, E.S., Garcia, S., Maroto-Valer, M., Barrio, J., Kvamsdal, H.M., URL https://papers.ssrn.com/sol3/papers.cfm?abstract_id=3366052 (accessed 1.6.20) 2019. MEA Consumption – ALIGN-CCUS: Comparative Long-Term Testing to Answer the Open Questions [WWW Document].
- Oyenekan, B.A., Rochelle, G.T., 2007. Alternative stripper configurations for CO₂ capture by aqueous amines. AIChE J. 53, 3144–3154, <http://dx.doi.org/10.1002/aic.11316>.

- Pohanish, R.P., 2012. Ethylene oxide. In: Pohanish, R.P. (Ed.), *Sittig's Handbook of Toxic and Hazardous Chemicals and Carcinogens*. Elsevier, pp. 1255–1259.
- Rochelle, G.T., 2009. Amine scrubbing for CO₂ capture. *Science* (80-) 325, 1652–1654, <http://dx.doi.org/10.1126/science.1176731>.
- Rochelle, G.T., 2012. Thermal degradation of amines for CO₂ capture. *Curr. Opin. Chem. Eng.*, <http://dx.doi.org/10.1016/j.coche.2012.02.004>.
- Rochelle, G.T., 2016. Conventional Amine Scrubbing for CO₂ Capture, in: *Absorption-Based Post-Combustion Capture of Carbon Dioxide*. Elsevier Inc., pp. 35–67, <http://dx.doi.org/10.1016/B978-0-08-100514-9.00003-2>.
- Skylogianni, E., Wanderley, R.R., Austad, S.S., Knuutila, H.K., 2019. Density and viscosity of the nonaqueous and aqueous mixtures of Methyl-diethanolamine and monoethylene glycol at temperatures from 283.15 to 353.15 K. *J. Chem. Eng. Data* 64, 5415–5431, <http://dx.doi.org/10.1021/acs.jced.9b00607>.
- Steffen, V., Silva, E.A. da, 2017. Steady-state modeling of equilibrium distillation. In: *Distillation - Innovative Applications and Modeling*. InTech, <http://dx.doi.org/10.5772/66833>.
- Tobiesen, F.A., Svendsen, H.F., 2006. Study of a modified amine-based regeneration unit. *Ind. Eng. Chem. Res.* 45, 2489–2496, <http://dx.doi.org/10.1021/ie050544f>.
- Vega, F., Sanna, A., Navarrete, B., Maroto-Valer, M.M., Cortés, V.J., 2014. Degradation of amine-based solvents in CO₂ capture process by chemical absorption. *Greenh. Gases Sci. Technol.*, <http://dx.doi.org/10.1002/ghg.1446>.
- Wagiulla, K.M., Soliman, M.A., 1993. Distillation column simulation by orthogonal collocation: efficient solution strategy. *J. King Saud Univ. - Eng. Sci.* 5, 17–40, [http://dx.doi.org/10.1016/S1018-3639\(18\)30569-5](http://dx.doi.org/10.1016/S1018-3639(18)30569-5).
- Wanderley, R.R., Knuutila, H.K., 2020. Mapping diluents for water-lean solvents: a parametric study. *Ind. Eng. Chem. Res.* 59, 11656–11680, <http://dx.doi.org/10.1021/acs.iecr.0c00940>.
- Wanderley, R.R., Yuan, Y., Rochelle, G.T., Knuutila, H.K., 2019. CO₂ solubility and mass transfer in water-lean solvents. *Chem. Eng. Sci.* 202, 403–416, <http://dx.doi.org/10.1016/j.ces.2019.03.052>.
- Wanderley, R.R., Pinto, D.D.D., Knuutila, H.K., 2020. Investigating opportunities for water-lean solvents in CO₂ capture: VLE and heat of absorption in water-lean solvents containing MEA. *Sep. Purif. Technol.* 231, 115883, <http://dx.doi.org/10.1016/j.seppur.2019.115883>.
- Wang, Z.M., Song, G.L., Zhang, J., 2019. Corrosion control in CO₂ enhanced oil recovery from a perspective of multiphase fluids. *Front. Mater.*, <http://dx.doi.org/10.3389/fmats.2019.00272>.
- Wong, M.K., Shariff, A.M., Bustam, M.A., 2016. Raman spectroscopic study on the equilibrium of carbon dioxide in aqueous monoethanolamine. *RSC Adv.* 6, 10816–10823, <http://dx.doi.org/10.1039/c5ra22926j>.
- Yang, J., Yu, W., Wang, T., Liu, Z., Fang, M., 2020. Process simulations of the direct non-aqueous gas stripping process for CO₂ desorption. *Ind. Eng. Chem. Res.* 59, 7121–7129, <http://dx.doi.org/10.1021/acs.iecr.9b05378>.
- Yaws, C.L., 2003. *Yaws' Handbook of Thermodynamic and Physical Properties of Chemical Compounds: Physical, Thermodynamic and Transport Properties for 5,000 Organic Chemical Compounds*. Knovel.
- Yaws, C.L., Satyro, M.A., 2015a. Vapor pressure – organic compounds. In: *The Yaws Handbook of Vapor Pressure*. Elsevier, pp. 1–314, <http://dx.doi.org/10.1016/b978-0-12-802999-2.00001-5>.
- Yaws, C.L., Satyro, M.A., 2015b. Vapor pressure – inorganic compounds. In: *The Yaws Handbook of Vapor Pressure*. Elsevier, pp. 315–322, <http://dx.doi.org/10.1016/b978-0-12-802999-2.00002-7>.
- Yuan, Y., Rochelle, G.T., 2018. CO₂ absorption rate in semi-aqueous monoethanolamine. *Chem. Eng. Sci.* 182, 56–66, <http://dx.doi.org/10.1016/j.ces.2018.02.026>.
- Yuan, Y., Rochelle, G.T., 2019. CO₂ absorption rate and capacity of semi-aqueous piperazine for CO₂ capture. *Int. J. Greenh. Gas Control.*, <http://dx.doi.org/10.1016/j.ijggc.2019.03.007>.
- Zhang, J., Qiao, Y., Agar, D.W., 2012. Intensification of low temperature thermomorphic biphasic amine solvent regeneration for CO₂ capture. *Chem. Eng. Res. Des.* 90, 743–749, <http://dx.doi.org/10.1016/j.cherd.2012.03.016>.
- Zhang, S., Shen, Y., Wang, L., Chen, J., Lu, Y., 2019. Phase change solvents for post-combustion CO₂ capture: principle, advances, and challenges. *Appl. Energy*, <http://dx.doi.org/10.1016/j.apenergy.2019.01.242>.
- Zhuang, Q., Clements, B., Dai, J., Carrigan, L., 2016. Ten years of research on phase separation absorbents for carbon capture: achievements and next steps. *Int. J. Greenh. Gas Control.*, <http://dx.doi.org/10.1016/j.ijggc.2016.04.022>.